

# AUXILIARY-WALL METHOD OF MEASURING HIGHLY INHOMOGENEOUS LOCAL HEAT FLUXES

V. K. Aslanyan, É. N. Voznesenskii,  
and V. I. Nemchenko

UDC 536.629.7

The auxiliary-wall method has been examined for measurement of highly inhomogeneous local heat-flux distributions. Equations are given for evaluating the components of the systematic error.

Measurement methods having high sensitivity and high spatial resolution are required in research on heat transfer between bodies and gas flows, particularly on models used in evacuated stationary systems. The auxiliary-wall method [1] and the stationary-gradient method [2] are common methods that meet the first requirement. Primary heat-flux transducers using such approaches now enable one to measure heat fluxes from  $5 \cdot 10^{-2}$  W/m<sup>2</sup> upward [3]. However, the resolution of such an instrument is at best  $3 \cdot 10^{-3}$  to  $5 \cdot 10^{-3}$  m, which is insufficient for use with models, particularly if there is a substantial change in the heat-flux density over distances comparable with the size of the transducer, or if the size of the latter is comparable with the size of the model itself, as often occurs in small or medium evacuated systems.

There is another way of applying the gradient method [4], in which one uses the feature that the tangential heat fluxes are small by comparison with the normal ones in a very thin layer of homogeneous material in which the inner side has a constant temperature and the outer one receives the inhomogeneous heat flux. Therefore, provided the thermal conductivity of the material is constant, the distribution of the incident heat flux is essentially proportional to the local temperature difference between the measurement surfaces, and therefore, one merely has to measure the distribution of the temperature difference. Microthermocouples make such measurements comparatively easy over areas of  $1 \cdot 10^{-5}$ – $1 \cdot 10^{-4}$  m<sup>2</sup>.

In vacuum systems, a largely unexpanded gas jet may encounter a flat obstacle [4], in which case the model may have a measuring layer in the form of a thin plate of Lucite equipped with absolute and differential copper-Constantan microthermocouples, with this plate cemented to a hollow copper body with epoxide resin, the copper being cooled internally by a liquid. The readings of the absolute thermocouples serve to monitor the temperature of the internal surface, while the differential microthermocouples measure the distribution of the temperature difference between the surfaces. Figure 1a shows a typical scheme for installation of differential microthermocouples. This system gives the highest sensitivity in measuring the thermo-emf, while at the same time it minimizes the error of measurement arising from distortion of the temperature distribution by the wires themselves, since the hot junction 5 is comparatively remote from the point of insertion of the wires into the layer.

The systematic error in the auxiliary-wall method is thus made up of the error due to the distortion of the temperature distribution by the thermocouples and the error arising from the lateral heat leak in the layer. We examine each of these contributions below.

We first consider the distortion occurring in the pattern; we assume the system of Fig. 1a for the differential microthermocouple on the basis that the thermal conductivity  $\lambda_1$  of either of the wires is much greater than the thermal conductivity  $\lambda$  of the material, while the thickness of the cement layer and the diameter  $d$  of the wire are much less than the thickness  $h$  of the measurement layer. This means that the effects of the cement layer can be neglected, as can the thermal perturbations arising from the horizontal parts of the wires. Consequently, we consider only the distortions arising from the normal parts of the wires passing through the layer, and the temperature distribution within each of the wires can be considered as one-dimensional by virtue of the above restrictions. Let the heat-flux density at the outer surface be constant, while the distances between the vertical parts of the wires are such that there are no overlapping regions of thermal perturbation. Then the relevant component of the error can be found by solving for the temperature deviations caused by a single wire:

---

Translated from *Inzhenerno-Fizicheskii Zhurnal*, Vol. 35, No. 1, pp. 29-40, July, 1978. Original article submitted March 25, 1976.

$$\begin{aligned} \frac{\partial^2 T}{\partial r^2} + \frac{1}{r} \frac{\partial T}{\partial r} + \frac{\partial^2 T}{\partial z^2} &= 0; \quad r > \frac{d}{2}; \quad 0 < z < h; \\ T(r, 0) &= T_1 = \text{const}; \quad r \geq \frac{d}{2}; \\ \lambda \frac{\partial T}{\partial z} \Big|_{z=h} &= q_w = \text{const}; \quad r > \frac{d}{2}; \\ T\left(\frac{d}{2}, z\right) &= T_{\text{in}}(z); \quad 0 \leq z \leq h; \\ |T(\infty, z)| &< \infty; \quad 0 \leq z \leq h, \end{aligned} \quad (1)$$

in which the temperature within the wire  $T_{\text{in}}(z)$ , in turn, is found by solving the following one-dimensional heat-conduction equation:

$$\begin{aligned} \frac{d^2 T_{\text{in}}}{dz^2} + \frac{4}{\lambda_1 d} q(z) &= 0; \quad 0 < z < h; \\ T_{\text{in}}(0) &= T_1; \quad \lambda_1 \frac{dT_{\text{in}}}{dz} \Big|_{z=h} = q_w, \end{aligned} \quad (2)$$

where  $q(z)$  is the density of the heat flux passing from the measurement layer into the conductor via the side surface:

$$q(z) = \lambda \frac{\partial T}{\partial r} \Big|_{r=\frac{d}{2}+0}.$$

Here  $r$  and  $z$  are cylindrical coordinates.

The known signs of  $q_w$  and  $q(z)$  have been utilized in inserting these into (1) and (2).

This case is not covered by any of the cases dealt with in the literature for such thermocouples [5, 6-8]; also, the perturbations are different from those produced by flattened thermocouples [9], since the latter relate to the extreme case  $d \gg h$ , apart from any restrictions on the boundary conditions.

We solve (1) with (2) analytically to obtain

$$\begin{aligned} T(r, z) &= T_1 + \frac{q_w}{\lambda} z + \frac{q_w}{\lambda} \left(1 - \frac{\lambda}{\lambda_1}\right) \frac{8h}{\pi^2} \sum_{n=0}^{\infty} \frac{(-1)^n}{(2n+1)^2} \times \\ &\times \left\{ \frac{K_0 \left[ (2n+1) \frac{\pi r}{2h} \right]}{K_0 \left[ (2n+1) \frac{\pi d}{4h} \right]} \sin(2n+1) \frac{\pi z}{2h} \right\} \left\| \left\{ 1 + \frac{8h}{\pi d} \cdot \frac{\lambda}{\lambda_1} \times \right. \right. \\ &\times \left. \left. \frac{1}{2n+1} \cdot \frac{K_1 \left[ (2n+1) \frac{\pi d}{4h} \right]}{K_0 \left[ (2n+1) \frac{\pi d}{4h} \right]} \right\} \right\}; \quad r \geq d/2; \\ T_{\text{in}}(z) &= T(d/2, z). \end{aligned}$$

Then we readily obtain the expression for the error of the method  $\varepsilon_1(r/h) = \frac{1}{q_w} \times \left[ \lambda \frac{T(r, h) - T_1}{h} - q_w \right]$ ,

due to the temperature-pattern distortion:

$$\begin{aligned} \varepsilon_1(r/h) &= -\frac{8}{\pi^2} \left(1 - \frac{\lambda}{\lambda_1}\right) \sum_{n=0}^{\infty} \frac{1}{(2n+1)^2} \times \\ &\times \left\{ \frac{K_0 \left[ (2n+1) \frac{\pi r}{2h} \right]}{K_0 \left[ (2n+1) \frac{\pi d}{4h} \right]} \right\} \left\| \left\{ 1 + \frac{8h}{\pi d} \cdot \frac{\lambda}{\lambda_1} \cdot \frac{1}{2n+1} \times \frac{K_1 \left[ (2n+1) \frac{\pi d}{4h} \right]}{K_0 \left[ (2n+1) \frac{\pi d}{4h} \right]} \right\} \right\}; \quad r \geq d/2; \\ \varepsilon_{1\text{in}} &= \varepsilon_1(d/2h), \end{aligned} \quad (3)$$

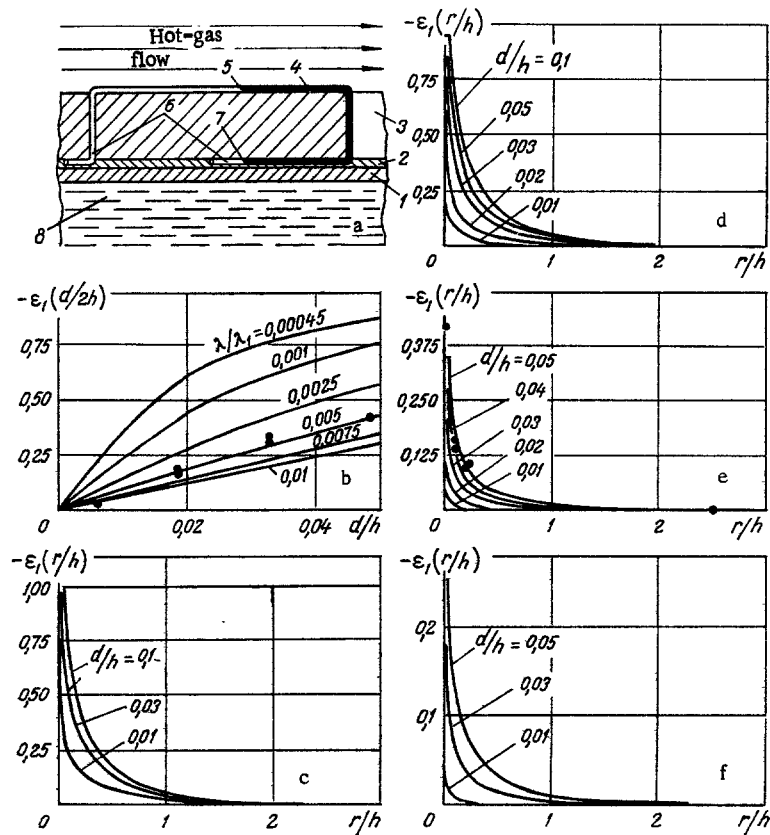


Fig. 1. Effects of heat-flux perturbation in measurement layer due to thermocouple wires on the error of heat-flux measurement: a) mode of installation of differential thermocouple [1) body of model; 2) cement joint; 3) measurement layer; 4, 6) Constantan and copper wires; 5, 7) hot and cold junctions of thermocouple; 8) thermostatic liquid]; b) dependence of  $\varepsilon_1$  in  $-\varepsilon_1(d/2h)$  on wire diameter for various  $\lambda/\lambda_1$  (the points are from  $\lambda/\lambda_1 \approx 0.0075$ ); c-f) effects of distance of hot junction from point of insertion of one of the wires on  $\varepsilon_1$  for various  $d/h$  and  $\lambda/\lambda_1$ : c)  $\lambda/\lambda_1 = 0$ ; d) 0.00045; e)  $\lambda/\lambda_1 = 0.0075$  (the points are from experiment for  $d/h = 0.49 \cdot 10^{-1}$ ); f)  $\lambda/\lambda_1 = 0.01$ .

where  $K_i(x)$  is a Macdonald function of order  $i$ .

Figure 1b-f shows computer calculations on  $\varepsilon_1(r/h)$  for various combinations of  $d/h$  and  $\lambda/\lambda_1$ ; the error  $\varepsilon_1(r/h)$  occurring on placing the hot junction near the point of insertion of one of the wires (as  $r \rightarrow d/2$ ) can be extremely large [ $\varepsilon_1(d/2h) = -1$  in the limiting case  $\lambda/\lambda_1 = 0$ ], and the measurement result in that case is quite incorrect. On the other hand, for  $r/h \geq 3.3$  and  $d/h \leq 1 \cdot 10^{-1}$  we have that  $\varepsilon_1(r/h) < 1 \cdot 10^{-3}$ , no matter what the value  $\lambda/\lambda_1 < 1$ ; i.e., the differential thermocouple should give a virtually unperturbed temperature-difference reading if placed in this way.

Measurements on the perturbation caused by the wires were performed with the above model having a Lucite layer of thickness  $1 \cdot 10^{-2}$  m, which was fitted at various points with normally placed Constantan wires of diameters  $4 \cdot 10^{-5}$  to  $0.49 \cdot 10^{-3}$  m. A copper wire of thickness  $3 \cdot 10^{-5}$  m was soldered to the end of each such wire, and these were brought out from both surfaces to a connection socket. Also, a Constantan rod of diameter  $0.49 \cdot 10^{-3}$  m had the ends of Constantan wires from the absolute copper-Constantan couples soldered to it (diameter of the wires  $3 \cdot 10^{-5}$  m), with the junctions placed on opposite sides of the layer, one opposite another, at distances from the axis of the rod that varied from one thermocouple to another.

The model was attached to the support in the working chamber, with the outside surface of the measurement layer parallel to the axis of the subsonic nozzle at a fixed distance from it. The heat flux at the surface of the model was set up by lateral interaction with the jet of hot air from the nozzle, which was largely unexpanded in that condition, and the model acted as an infinite flat baffle in relation to the jet. The model could

be displaced with the support system to bring the hot junctions of all thermocouples, in turn, to the same distance from the end of the nozzle (to the point where the heat flux along the surface of the baffle varied comparatively little), which ensured that each junction had identical external heat-transfer conditions. The readings of the differential thermocouples were taken with an R37-1 potentiometer of class 0.01, and then the values of  $\varepsilon_1(d/2h)$  and  $\varepsilon_1(r/h)$  were calculated. The maximum error  $\varepsilon_1$  was then essentially dependent on the error of thermocouple calibration and did not exceed 0.035.

Parts b and e of Fig. 1 show the results; the observed points in Fig. 1b in the main lie above the corresponding theoretical curve, since, in fact, there was not ideal thermal contact between the plate and the wires fitted in it. Figure 1e shows results that, apart from the initial point, agree well with the theoretical solution.

Therefore, thermocouples can be used as in Fig. 1a with this analysis to determine the distribution of the temperature difference across the layer with a given accuracy.

One can convert to the distribution of the heat fluxes by examining the thickness of the measurement layer that will provide an acceptable level of lateral heat leakage on account of the variation in the external heat flux along the outside surface.

The effects of lateral heat leakage on the error of measurement have been examined previously in the main for nonstationary means of measuring heat fluxes [10, 11]. Only certain particular cases have been considered for the auxiliary-wall method [1, 4].

Here we derive relationships for the general case that provide preliminary definition of the layer thickness and which can also be used for calculating the error arising from heat leakage during such measurements.

We assume that the thickness of the layer is small by comparison with the principal radii of curvature of the surface; then the temperature distribution within the layer is described by the Laplace equation in the form

$$\frac{\partial^2 T}{\partial x^2} + \frac{\partial^2 T}{\partial y^2} + \frac{\partial^2 T}{\partial z^2} = 0, \quad (4)$$

where  $x$ ,  $y$ , and  $z$  are orthogonal coordinates as follows:  $x$  and  $y$  lie along the internal (isothermal) surface of the layer, while  $z$  lies along the normal to it toward the outer surface.

The following are the boundary conditions at the surfaces of the layer:

$$T(x, y, 0) = T_1 = \text{const}; \quad \lambda \left. \frac{\partial T}{\partial z} \right|_{z=h} = q_w(x, y), \quad (5)$$

and the distribution  $q_w(x, y)$  of the heat-flux density at the outer surface is assumed to be continuous.

We integrate (4) with respect to  $z$  using (5) to obtain an exact expression for the local error  $\varepsilon_2$  arising from lateral heat leakage:

$$\begin{aligned} \varepsilon_2 &= \frac{1}{q_w(x, y)} \left[ \lambda \frac{T_2 - T_1}{h} - q_w(x, y) \right] = \\ &= \frac{\lambda}{q_w(x, y)} \left[ \int_0^h \Delta' T dz - \frac{1}{h} \int_0^h dz \int_0^z \Delta' T d\xi \right]. \end{aligned} \quad (6)$$

Here

$$T_2 = T(x, y, h); \quad \Delta' = \frac{\partial^2}{\partial x^2} + \frac{\partial^2}{\partial y^2}.$$

We suppose that the layer is so thin that the longitudinal heat fluxes are small by comparison with the transverse ones; then the  $z$  distribution of the temperature within the layer is approximately linear:

$$T(x, y, z) - T_1 \approx (T_2 - T_1) \frac{z}{h}$$

and we use this representation with (6) to obtain the following equations for  $\varepsilon_2$ :

$$\varepsilon_2 \approx \frac{\lambda h}{3} \cdot \frac{\Delta' (T_2 - T_1)}{q_w(x, y)} \approx \frac{h^2}{3} \cdot \frac{\Delta' (T_2 - T_1)}{T_2 - T_1}. \quad (7)$$

Formula (7) allows one to calculate  $\varepsilon_2$  from the measurements. If  $q_w(x, y)$  is doubly differentiable, we can give the following form for (7):

$$\varepsilon_2 \approx \frac{h^2}{3} \cdot \frac{\Delta' q_w(x, y)}{q_w(x, y)}, \quad (8)$$

which was used subsequently in comparing the approximate and exact values of the error arising from lateral leakage. This comparison was performed on models in order to test the relationships.

Equations (7) and (8) are of asymptotic type, and the error should be directly related to the thickness of the layer by virtue of the assumptions made.

These equations apply for a layer in which the side surface is thermally insulated; if the boundary conditions at the sides are other than these, it is still permissible to use the equations for parts of the layer at distances greater than about  $5h$  from the edges [3].

From (7) and (8) we obtain a consequence of considerable practical importance: If the layer is thin, the error arising from lateral heat leakage is proportional to the square of the thickness of the layer, the order of the quantity being

$$\varepsilon_2 \sim (h/L_*)^2, \quad (9)$$

where  $L_*$  is the characteristic linear dimension of the nonuniformity in the heat flux.

This means, first of all, that a thin layer should be defined as a layer such that  $(h/L_*)^2 \ll 1$ ; secondly, this condition indicates the choice of layer in designing a model.

The equations that approximate  $\varepsilon_2$  have been checked theoretically and by experiment; in the first case, we compared the exact values  $\varepsilon_{2e}$  derived from analytical solution of model two-dimensional steady-state problems with the approximate ones  $\varepsilon_{2a}$  derived from (8). The heat-flux distribution at the outer surface of a plate of length  $L$  (planar case) or of a flat disk of radius  $R$  (axially symmetrical case) was given as a certain function; the side surfaces (at  $x=0$  and  $x=L$  in the planar case or at  $r=R$  in the axially symmetrical case) were considered as thermally insulated. The solution was determined by separating the variables.

Parts a and b of Fig. 2 show  $\varepsilon_{2e}$  for a planar case with the heat flux given by

$$q_w(\bar{x}) = \left(\frac{A\bar{x}}{2}\right)^2 \exp(-A\bar{x} + 2), \quad (10)$$

where  $\bar{x}=x/L$  and  $A$  take the values 20 and 40, respectively, for  $\bar{h}=h/L=0.01, 0.03,$  and  $0.05$ ; the distributions of (10) are also shown.

Figure 2c shows analogous data for the axially symmetrical case, in which the heat-flux distribution was described by

$$q_w(\bar{r}) = \frac{1}{1.4028} [0.4028 + J_0(3.8317 \bar{r})], \quad (11)$$

where  $\bar{r}=r/R$  and  $J_0(x)$  is a Bessel function of the first kind of zero order; here  $\bar{h}=h/R=0.02, 0.06,$  and  $0.1$  and for comparison of  $q_w(\bar{r})$  we show the graph for  $\lambda(\Delta T_w/h)=\lambda[(T_2-T_1)/h]$  for  $\bar{h}=0.1$ .

It is clear that  $\varepsilon_2$  everywhere decreases as the layer becomes thinner, apart from points where the incident heat flux is zero; i.e., the longitudinal heat fluxes in the layer decrease, and the local values of  $\lambda(\Delta T_w/h)$  and  $q_w(\bar{x})$  or, respectively,  $q_w(\bar{r})$  become similar, this occurring the more rapidly, the smoother the distribution of the heat flux (compare parts a and b of Fig. 2). Consequently, one is justified in approximating the transverse temperature distributions in the layer by linear functions for  $h \rightarrow 0$ , and there should be a tendency for the approximate values to approach the exact ones asymptotically. Table 1 gives a clear confirmation of this.

These comparisons also show that (9) gives the correct order for  $\varepsilon_2$  in the neighborhood of the peak  $q_w(\bar{x}) \cdot [q_w(\bar{r})] = q_{\max}$  for the entire range in  $\bar{h}$ ; as our  $L_*$  we took the least of the distances from the  $q_{\max}$  point to the point at which  $q_w(x)[q_w(\bar{r})]=0.1 q_{\max}$ .

The scope for using (7)-(9) in practice for estimating  $\varepsilon_2$  was examined for the interaction of a highly compressed hot-air jet from a subsonic nozzle with a planar baffle in an evacuated system. The measurement layers on the model were Lucite plates of various thicknesses ( $1 \cdot 10^{-3}$  to  $4.4 \cdot 10^{-3}$  m), which were fitted with differential copper-Constantan thermocouples. These were installed as in Fig. 1a, and (3) then indicated that  $\varepsilon_1 < 0.1\%$ ; the thickness of the layer was chosen by trial to be such that the lateral heat leakage near the  $q_{\max}$  point was unimportant, and then  $\varepsilon_2$  was estimated for this thickness. Figure 2d shows the experimental results; the abscissa is the dimensional thickness and the ordinate is a quantity proportional to the ratio of

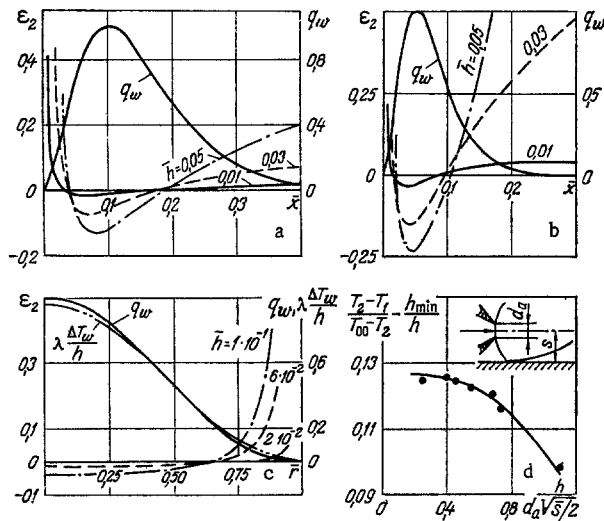


Fig. 2. Heat leakage in the measurement layer for various model conditions and for the working conditions: a, b) model planar stationary case for a layer with a heat-flux distribution of the form of (10) with A of 20 and 40, respectively; c) the same for the axially symmetrical case with a heat flux of the form of (11); d) ratio of the measured heat flux to the actual flux at a point  $q_{\max}$  as a function of the dimensionless thickness of the measuring layer for a highly condensed air jet interacting with a flat obstacle.

TABLE 1. Comparison of  $\varepsilon_{2e}$  and  $\varepsilon_{2a}$  and Test on the Linear Approximation for Transverse Temperature Distribution in a Layer for the Axially Symmetrical Case with a Heat Flux of the Form of (11)

$\bar{r}$	$\bar{h}$	$\frac{\partial T}{\partial z} \Big _{z=h} / \frac{\partial T}{\partial z} \Big _{z=0}$	$\varepsilon_{2e}$	$\varepsilon_{2a}$	$\varepsilon_{2a}/\varepsilon_{2e}$
0	0,10	1,0519	$-3,2950 \cdot 10^{-2}$	$-3,4887 \cdot 10^{-2}$	1,0588
	0,06	1,0188	$-1,2299 \cdot 10^{-2}$	$-1,2559 \cdot 10^{-2}$	1,0212
	0,02	1,0022	$-1,3922 \cdot 10^{-3}$	$-1,3955 \cdot 10^{-3}$	1,0024
0,261	0,10	1,0475	$-2,9924 \cdot 10^{-2}$	$-3,2062 \cdot 10^{-2}$	1,0715
	0,06	1,0172	$-1,1303 \cdot 10^{-2}$	$-1,1542 \cdot 10^{-2}$	1,0212
	0,02	1,0019	$-1,2791 \cdot 10^{-3}$	$-1,2825 \cdot 10^{-3}$	1,0026
0,496	0,10	1,0293	$-1,9020 \cdot 10^{-2}$	$-2,0145 \cdot 10^{-2}$	1,0592
	0,06	1,0108	$-0,7094 \cdot 10^{-2}$	$-0,7252 \cdot 10^{-2}$	1,0223
	0,02	1,0012	$-0,8032 \cdot 10^{-3}$	$-0,8050 \cdot 10^{-3}$	1,0032
0,757	0,10	0,9200	$5,8084 \cdot 10^{-2}$	$6,1510 \cdot 10^{-2}$	1,0590
	0,06	0,9685	$2,1677 \cdot 10^{-2}$	$2,2139 \cdot 10^{-2}$	1,0213
	0,02	0,9963	$2,4519 \cdot 10^{-3}$	$2,4599 \cdot 10^{-3}$	1,0032

the measured heat flux to the actual flux. The distance  $s$  from the axis of the jet to the surface of the baffle was set as  $\bar{s} = 2s/d_a = 12$ , while the diameter of the exit section of the nozzle was  $d_a = 1.65 \cdot 10^{-3}$  m,  $h_{\min} = 1 \cdot 10^{-3}$  m, and the stagnation temperature of the jet was  $T_{00} = 400^\circ\text{K}$ . The form of the experimental curve shows that the lateral heat leakage near the  $q_{\max}$  point is slight for  $h \leq h_{\min}$ , while (9) shows the error due to lateral heat leakage in the layer is about 1.5% for  $h \approx h_{\min}$ , which is in good agreement with the observed curve in this region. The results of [4] were used in determining the characteristic scale of the nonuniformity in the heat flux.

A complete study requires examination of a discontinuous heat-flux distribution; the lateral heat leakage is always considerable at the point of discontinuity (apart from the limiting case of an infinitely thin layer), so it is important to examine the scale of the region around the discontinuity outside of which the effect can be neglected.

We performed a numerical parametric study of a model steady-state case for the above planar and axially symmetrical circumstances with the heat-flux distribution at the outer surface of a step form (this made it possible to examine the effects of the discontinuity in pure form). We found that the lateral heat leakage due to the discontinuity became essentially zero at a distance of  $3h$  from the discontinuity, and the error of the method

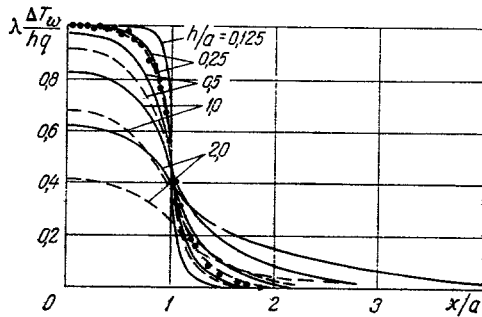


Fig. 3

Fig. 3. Local temperature differences between the surfaces of the measurement layer for a heat flux with a step distribution; the solid and dashed curves are from the theory for the planar and axially symmetrical cases, respectively (the solid lines are for  $h/L = 2 \cdot 10^{-2}$  and the dashed lines for  $h/R = 1 \cdot 10^{-2}$ ); the points are from experiment for the planar case with  $h/a = 0.24$ .

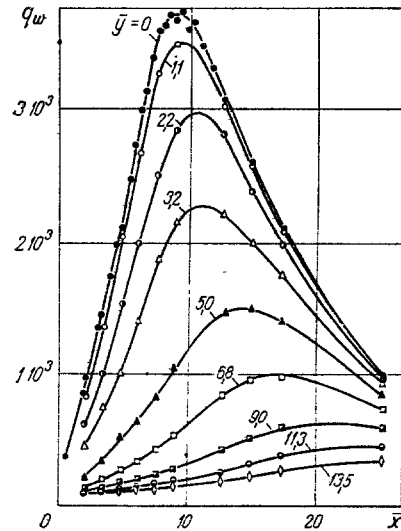


Fig. 4

Fig. 4. An example of a convective heat-flux distribution  $q_w$  ( $W/m^2$ ) at a flat obstacle for natural interaction with a highly condensed hot-air jet.

arising from the discontinuity was less than 1% of the discontinuity itself. Figure 3 shows the calculations and a check experiment for the planar case ( $a$  is the geometrical parameter that defines the linear dimensions of the region of action of the heat flux, while  $q$  is the height of the step in the heat-flux distribution). A nearly square heat-flux distribution was set up by a special radiation source, which was moved along the blackened surface of the layer (Lucite,  $h = 0.95 \cdot 10^{-3}$  m), which contained the differential microthermocouples. Theory and experiment were in good agreement for  $x/a < 1$ , but there were some discrepancies between the two for  $x/a > 1$  on account of the deviation of the actual real distribution from square.

This means that the auxiliary-wall method can be used with an accuracy sufficient for practical purposes to measure the heat-flux distribution even in the presence of a discontinuity, apart from areas less than  $3h$  from the point of discontinuity.

Therefore, a thin measuring layer with microwires can be used to reduce the systematic error to within acceptable limits, while substantially improving the spatial resolution and thereby making it possible to measure highly inhomogeneous steady-state local heat-flux distributions.

Figure 4 shows the distribution of convective heat fluxes on a flat-baffle model, which was placed in an evacuated tube within a hot-air jet near the nozzle and parallel to the axis. The Lucite measurement layer had a thickness of  $0.9 \cdot 10^{-3}$  m, while the wires in the differential microthermocouples (copper-Constantan) had a diameter of  $2 \cdot 10^{-5}$  m. The spatial resolution was then about  $5 \cdot 10^{-5}$  m. The measurements were made under the following conditions: pressure and stagnation temperature in the jet, respectively,  $P_0 = 6.33 \cdot 10^4$  Pa and  $T_0 = 763$  K;  $M_a = 3.65$ ;  $P_0/P_\infty = 2.2 \cdot 10^4$  to  $2.5 \cdot 10^4$  ( $P_\infty$  is the pressure in the working chamber outside the jet),  $T_1 = 295$  K;  $d_{ae} = 4.33 \cdot 10^{-3}$  m, where the latter is the effective diameter of the end of the nozzle; angle of the nozzle cone  $20^\circ$ ; and distance from the surface of the baffle to the axis of the jet  $2s/d_{ae} = 4.5$ . Here  $M_a$  and  $d_{ae}$  were determined in accordance with the recommendations of [12]. The distribution of  $q_w$  was plotted as a function of the dimensionless Cartesian coordinates  $\bar{x} = 2x/d_{ae}$  and  $\bar{y} = 2y/d_{ae}$  on the surface, where  $x$  was reckoned from the plane of the end of the nozzle along the line of intersection of the surface of the baffle with the plane perpendicular to it passing through the axis of the nozzle.

Qualitatively speaking, the pattern of Fig. 4 is similar to that of [4] for the case  $M_a = 1$ , but it differs from the latter in that the fall in the heat flux from the  $q_{w,max}$  point in the longitudinal direction was less rapid than that in the transverse direction. It seems that this difference is due to the reduction in the transverse size of the jet as  $M_a$  increases.

The estimates show that  $\varepsilon_2$  for the  $q_w$  distribution of Fig. 4 was about 0.25%, while  $\varepsilon_1$  was less than 0.1%. The absolute error in calibrating the thermocouples did not exceed 1.5%, while the error in determining the thermal conductivity of the lucite was  $\pm 5\%$ . Therefore, the overall error in measuring  $q_w$  was about  $\pm 5.5\%$ .

#### NOTATION

$x, y, z$ , Cartesian coordinates;  $r, z$ , cylindrical coordinates;  $\xi$ , integration variable;  $h$ , thickness of measuring layer, m;  $h_{\min} = 1 \cdot 10^{-3}$  m;  $d$ , diameter of thermocouple wire, m;  $d_a, d_{ae}$ , end diameter and effective end diameter of nozzle, m;  $s$ , distance from jet axis to wall (Fig. 2d), m;  $L_*$ , characteristic linear dimension of heat-flux nonuniformity, m;  $L, R$ , length of plate and radius of disk in two-dimensional models for measuring layer, m;  $a$ , region of stepped heat flux, m;  $\bar{x} = x/L$  in (10) and in Fig. 2a, b;  $A$ , parameter in (10);  $K_i(x), J_0(x)$ , cylindrical functions;  $\exp x$ , exponential function;  $T$ , temperature, °K;  $T_{in}$ , temperature inside a normal part of thermocouple, °K;  $T_1, T_2$ , temperatures of internal and external sides of measuring layer, respectively, °K;  $\Delta T_w = T_2 - T_1$ ;  $T_{00}$ , jet stagnation temperature, °K;  $q$ , height of step in discontinuous heat-flux distribution,  $W/m^2$ ;  $q(z)$ , heat flux from the measuring layer through side surface of normal thermocouple section,  $W/m^2$ ;  $q_w$ , heat-flux density at the outer surface of measuring layer,  $W/m^2$ ;  $q_{\max}$ , maximum  $q_w$ ;  $\lambda, \lambda_1$ , thermal conductivities of the measuring layer and thermocouple, respectively,  $W/m \cdot \text{deg}$ ;  $P_0, P_\infty$ , pressures in the mixing chamber and working chamber of the tube outside the jet, Pa;  $M_a$ , value of  $M$  at end of nozzle;  $\varepsilon_1$ , error due to distortion of the temperature distribution by the thermocouples;  $\varepsilon_2$ , error due to heat propagation in the measuring layer;  $\varepsilon_{2e}, \varepsilon_{2a}$ , exact and approximate values of  $\varepsilon_2$ .

#### LITERATURE CITED

1. O. A. Gerashchenko, Principles of Heat Measurement [in Russian], Naukova Dumka, Kiev (1971).
2. N. D. Danilov, in: Dynamics of Thermal Processes [in Russian], Naukova Dumka, Kiev (1972).
3. Hedger, Jr., Rev. Sci. Instr., No. 11 (1965).
4. É. N. Voznesenskii and V. I. Nemchenko, in: Proceedings of the 18th Moscow Technical Physics Conference 1972. Aerial Mechanics and Control Processes Series [in Russian], Moscow (1973).
5. V. N. Popov, Teplofiz. Vys. Temp., 4, No. 2 (1966).
6. A. A. Shershnev and É. B. Mikhailov, Izv. Vyssh. Uchebn. Zaved., Priborostr., 18, No. 3 (1975).
7. J. V. Beck, Teploperedacha, 84, No. 2 (1962).
8. J. V. Beck and H. Hurwicz, J. Heat Transfer, Trans. ASME, Ser. C, 82, No. 1 (1960).
9. O. A. Gerashchenko and V. G. Fedorov, Techniques in Heat-Engineering Experiments [in Russian], Naukova Dumka, Kiev (1964).
10. G. I. Maikapar, Tr. Tsentr. Aéro-Gidrodinam. Inst., No. 1106 (1968).
11. George and Rheinecke, Raketn. Tekh. Kosmonavt., 1, No. 8 (1963).
12. N. I. Yushchenkova, S. A. Lyzhnikova, and V. I. Nemchenko, in: Transport Phenomena in Low-Temperature Plasmas [in Russian], Nauka i Tekhnika, Minsk (1969).